WELDING RESEARCH

SUPPLEMENT TO THE WELDING JOURNAL, JULY, 1983

Sponsored by the American Welding Society and the Welding Research Council

Friction Weld Ductility and Toughness As Influenced by Inclusion Morphology

Differences in properties between inertia and continuous drive welds appear associated with microstructural variations resulting from different heat inputs and cooling rates for the two process variations

BY B. J. EBERHARD, B. W. SCHAAF, JR., AND A. D. WILSON

ABSTRACT. Friction welding consistently provides high strength, freedom from fusion defects, and high productivity. However, friction welds in carbon steel exhibit impact toughness and bend ductility that are significantly lower than that of the base metal. The inclusion content and morphology were suspected to be major contributors to the reduction in weld ductility. For this reason, four electric furnace steels—three types of ASTM A516 Grade 70, and an ASTM A737 Grade B steel—were investigated. Friction welds were made by both the inertia and direct drive process variations and the welds evaluated.

It was shown that friction welds of inclusion-controlled steels exhibited much improved toughness and bend ductility. Upper shelf impact energy was equivalent to or greater than that of the base metal in the short transverse direction. The transition temperature range for all four materials was shifted to higher temperatures for both types of friction welds. Under the conditions of this test, the direct drive friction welds showed a greater shift than the inertia friction welds.

The ductility and toughness of welds in A737 Grade B steel were superior to welds in A516 Grade 70 steels, reflecting the superior properties of the base metal. Welds of the A737 material had usable Charpy V-notch impact toughness of 20 to 30 ft-lb (27 to 41 J) at temperatures as low as −40°F (−40°C).

All the welds had an acicular structure. The differences in properties between the inertia and direct drive friction welds appear associated with microstructural variations. These variations resulted from the different heat inputs and cooling rates of the two process variations. The work described in this paper demonstrates the beneficial effects of inclusion control on toughness and ductility. In addition, it also indicates that additional improvements may be attainable through control of the as-welded microstructure by process manipulation.

Introduction

This program was undertaken to determine if the recently developed inclusion controlled steels are capable of enhancing the bend ductility and fracture toughness of friction welded joints. The work was done cooperatively by members of the AWS C6 Friction Welding Committee. The specific objective of this program was to investigate the suitability of friction welding to meet the extreme demands of shipping container fabrication (Ref. 1).—i.e., Charpy V-notch impact of 15 ft-lb (20J) at −40°F (−40°C) and 180 deg bend ductility at room temperature. These demands are imposed to ensure the safe handling of nuclear materials despite all the mishaps that can be imagined.

Friction welding is a candidate process being investigated at the Savannah River Plant for remotely encapsulating 2 ft (0.6 m) diameter × 10 ft (3.0 m) long canisters of nuclear waste (stabilized by solid solution in glass) in a carbon steel overpack. Rugged, massive equipment would be required to hold, spin, and friction weld the lid in correct alignment with the overpack body (containing the vitrified waste form). This process is ideal for remote welding. Once the pieces to be welded have been placed in the friction welding machine, the machine does the rest simply, dependably, and automatically.

Friction welding is often used to join materials where the consistently good strength of solid-state welds is required. Yet, like flash welding and induction, upset, or pressure gas welding, the transverse bend ductility and fracture toughness weld properties are not particularly good. Work conducted during and after World War II suggested that oxides formed during welding, and those already present in the materials being welded, might be the cause of the low ductility and fracture toughness of these solid-state welds (Ref. 2, 3, 4). The presence of "flat spots" or "penetrators" in test fractures of older forms of solid-state welded butt joints and limitations that are placed on weld ductility and toughness are thought to be manifestations of brittle inclusions.

Preliminary work to explore the feasibility of friction welding of large diameter

---

Paper sponsored by the AWS C6 Committee on Friction Welding and presented at the 63rd AWS Annual Convention in Kansas City, Missouri, during April 25-30, 1982.

B. J. EBERHARD is Staff Engineer, E. I. du Pont de Nemours & Co., Inc., Aiken, South Carolina, and B. W. SCHAAF, JR., is a Consultant for E. I. du Pont de Nemours in Wilmington, Delaware; A. D. WILSON is Senior Research Engineer, Lukens Steel Company, Coatesville, Pennsylvania.

Table 1—Testing Materials

Plate identification[(a)]	Rolling characteristics: Reduction Ratio[(b)]	Rolling characteristics: L/T Ratio[(c)]
A516 CON	18.0	3.0
A516 ESR	60.0	30.8
A516 CaT	18.0	2.8
A737 CaT	18.0	2.0

(a) CON—conventional electric furnace practice; ESR—electroslag remelted; CaT—Calcium treated electric furnace practice.

(b) Ratio of original as-cast thickness to final plate thickness.

(c) $\frac{\text{(Final plate length)} \times \text{(Initial slab width)}}{\text{(Initial slab length)} \times \text{(Final slab width)}}$

pipe resulted in unsatisfactory bend ductility and impact toughness for this container application. Eighteen in. (45.7 cm) OD × 0.5 in. (12.7 mm) wall sections of ASTM A106 pipe were friction welded and evaluated. These welds failed the 180 deg bend test by cracking along the flow direction of the upset weld metal—Fig. 1. These cracks were shown to be associated with nonmetallic inclusions in the steel pipe.

It is hypothesized that the same inclusions in steel plate which reduce through-thickness (short transverse) ductility and toughness, thereby promoting lamellar tearing, reduce the ductility and toughness of friction welds. Through-thickness properties of plates are reduced by the flattening and elongation of inclusions during hot rolling. In friction welding the through-thickness inclusions are rotated into the zone of coalescence by the plastic flow which produces the weld and its collar of upset. This rotation of inclusions is apparent in cross section as flow lines in a macrograph from a section through a friction weld—Fig. 1.

The AWS C6 program was conducted on three inclusion quality levels of ASTM A516 Grade 70 steel and a microalloyed A737 Grade B steel; all four are pressure vessel steels that were candidate materials for this canister application. Plates, each 0.5 in. (12.7 mm) thick, were rolled and welded into 5 in. (127 mm) OD pipe to facilitate friction welding and to better simulate the application.

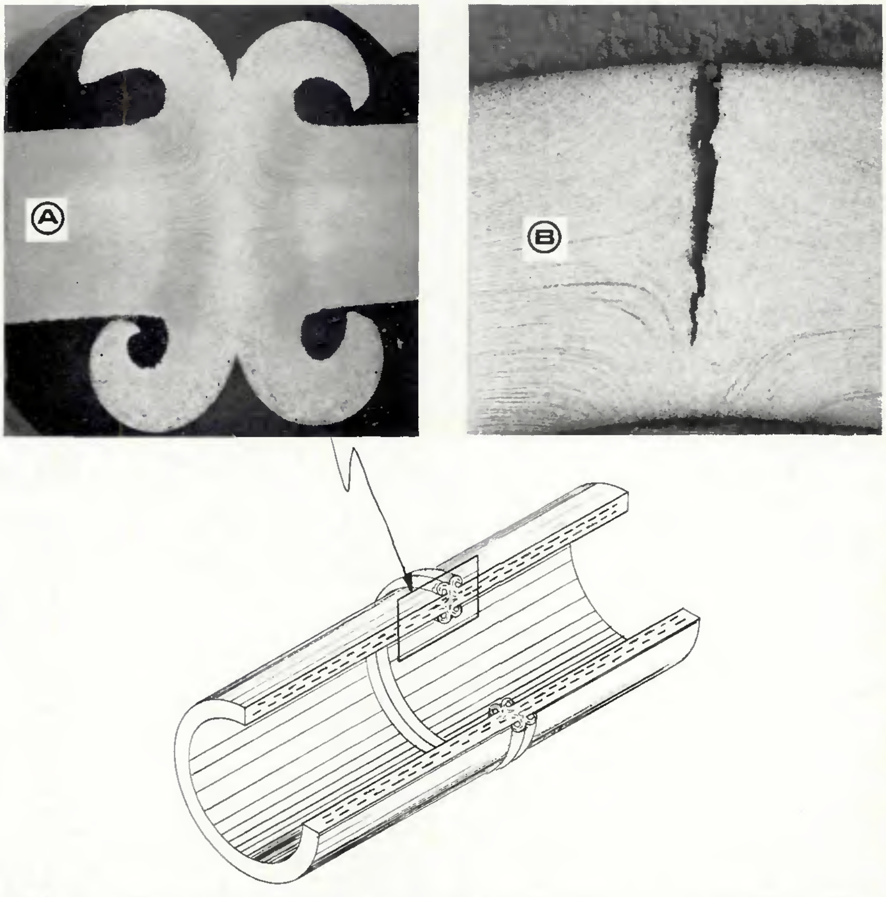

Fig. 1—Formation of a friction weld in pipe showing: A—metal flow; B—tendency for cracks to propagate in the flow direction along planes of weakness such as lamellar inclusions and laps

The Base Materials

Four individual heats of steel were evaluated as 0.5 in. (12.7 mm) thick plate and used in the friction welding experiments. Conventional electric furnace practice (CON), electroslag remelted (ESR), and calcium treated electric furnace practice (CaT) heats were each produced of A516, while the A737 heat was produced by CaT. All four heats were produced to aluminum killed fine grain practice. Table 1 summarizes the identification, steelmaking, and rolling practices used for these plates. The chemical compositions of the base metals are given in Table 2.

Inclusions

The various steelmaking practices used in producing the plates resulted in nonmetallic inclusion structures typical of each practice (Ref. 5). The CON steel

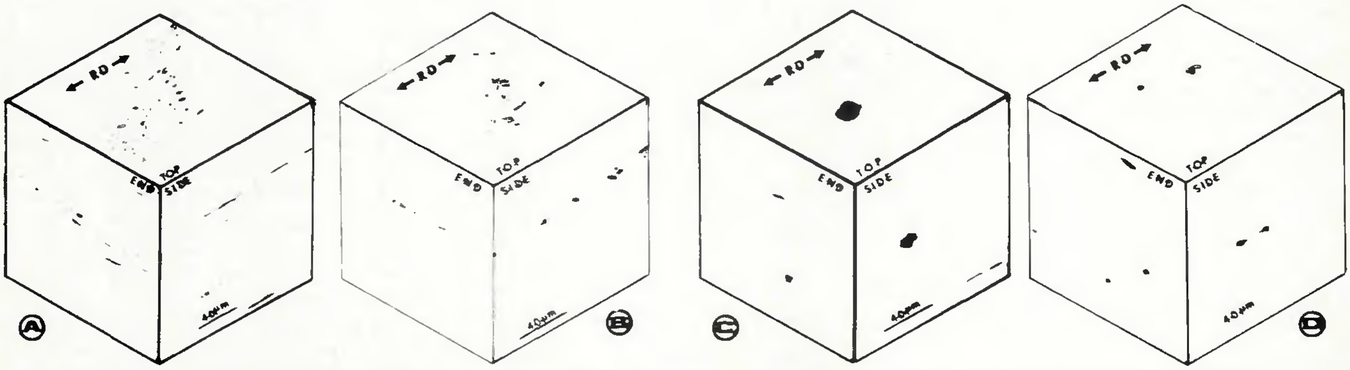

Fig. 2—Composite micrographs showing: A—manganese sulfide inclusion shape and distribution of A516 CON; B—clusters of aluminum oxide inclusions in A516 CON; C—calcium modified (darker) and smaller (gray, lens shaped) manganese sulfide inclusions of the A516 CaT steel; D—fewer and smaller inclusions in the A516 ESR steel resulting from the higher solidification rate achieved in this refining process. Unetched, X500 (reduced 49% on reproduction)

Table 2—Base Metal Analysis, %

Material	C	S	Mn	P	Cu	Si	Ni	Cr	Mo	Cb
A516 CON	0.24	0.025	1.06	0.006	0.22	0.27	0.25	0.12	0.06	NA
A516 ESR	0.20	0.006	1.17	0.007	0.16	0.22	0.14	0.08	0.03	NA
A516 CaT	0.21	0.004	0.97	0.008	0.32	0.24	0.09	0.11	0.02	NA
A737 CaT	0.12	0.005	1.32	0.010	0.18	0.17	0.10	0.12	0.02	0.023

Table 3—Base Metal Tensile Properties[(a)]

Material	Orient.	YS		UTS		El, %	RA, %
		ksi	(MPa)	ksi	(MPa)		
A516 CON[(b)]	L	57.3	(395)	84.5	(583)	29.4	65.8
	T	56.1	(387)	84.4	(582)	27.4	59.6
	S	(d)		79.5	(548)	(d)	18.0
A516 ESR[(b)]	L	57.9	(399)	83.3	(574)	30.6	71.1
	T	58.0	(400)	83.5	(576)	28.7	63.7
	S	(d)		80.3	(554)	(d)	47.3
A516 CaT[(b)]	L	55.5	(383)	82.0	(565)	29.5	68.8
	T	55.4	(382)	82.5	(569)	30.4	63.4
	S	(d)		64.9	(447)	(d)	45.5
A737 CaT[(c)]	L	70.2	(484)	82.7	(570)	32.8	80.8
	T	70.4	(485)	83.2	(574)	28.5	73.4
	S	(d)		78.6	(542)	(d)	66.7

(a) Orientations: L—longitudinal; T—transverse; S—through-thickness. Properties: YS—yield strength, 0.2% offset; UTS—ultimate tensile strength; El—elongation; RA—reduction of area.
(b) Average of 4 tests L & T orientations; average of 10 tests in S orientation.
(c) Average of 2 tests L & T orientations; average of 5 tests in S orientation.
(d) Could not be obtained because of limited gauge length of specimen.

contained Type II, manganese sulfide inclusions which had been flattened and elongated during hot rolling as shown in Fig. 2A. Additionally, clusters of aluminum oxide inclusions were present in the CON steel as noted in Fig. 2B.

Calcium treatment by injecting calcium compounds into the molten steel in the ladle minimizes both inclusion types through desulfurization and inclusion shape control. The significant difference in sulfur level between the CON steel and CaT steels is noted in Table 2. A majority of the remaining inclusions in the CaT steels are modified by calcium to form inclusions resistant to deformation during hot rolling. Manganese sulfide inclusions that remain in CaT steels also tend to be smaller. These inclusion varieties are shown in Fig. 2C.

ESR steels also are improved by desulfurization, but there also are additional benefits. The ESR steel was refined by remelting through a molten flux and then solidified in a water-cooled copper mold. This faster cooling rate tends to result in smaller nonmetallic inclusions—Fig. 2D.

Microstructures

Type A516-70 is a normalized C-Mn steel with specified minima of 38 ksi (262 MPa) yield and 70 ksi (483 MPa) ultimate tensile strengths. A737B is a C-Mn-Cb steel that is microalloyed with columbium, and for this application the normalized heat treatment was evaluated with the specified minima of 50 ksi (345 MPa) yield and 70 ksi (483 MPa) ultimate tensile strengths. It has been well established that the strength and toughness properties of A737 are superior to those of A516 (Ref. 6).

The improved A737 properties came about because the 0.05 wt-% maximum Cb addition results in fine columbium carbonitride precipitation; this retards austenitic grain growth during hot rolling and subsequent heat treatment cycles. The fine grain size leads to excellent transition toughness properties and higher yield strengths. Also, because of the yield strength improvement obtained from the fine grain size and higher manganese content, a lower carbon content can be utilized for A737 than is used for A516. The decreased level of carbides in A737 leads to improved ductility and upper shelf and transition toughness.

It was felt that the Cb carbonitride precipitates in A737 might help in improving the resistance to heat-affected zone degradation during friction welding. However, this benefit could only be realized if the temperatures reached in these solid-state weld processes were not excessive. A comparison of the microstructures of A516 and A737 plates is presented in Fig. 3. The finer grain size and lower levels of pearlite in the A737 steel are evident.

Tensile Properties

The base metal tensile properties for the four subject plates (before fabrication into pipe) are given in Table 3. Both longitudinal (L), transverse (T), and through-thickness (S) testing orientations were evaluated. The L and T orientations were evaluated using standard 0.252 in. (6.4 mm) diameter specimens, while the S orientation results were established using miniature, buttonhead specimens with a 0.112 in. (2.8 mm) gauge diameter.

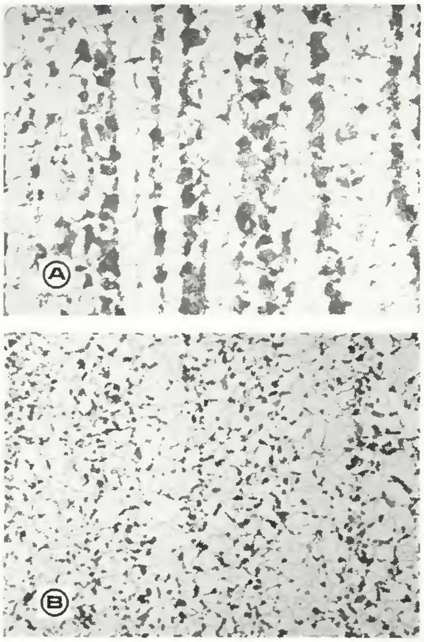

Fig. 3—Comparison of grain size and pearlite content of A516 Grade 70 and A737 Grade B steels: A—A516 CaT; B—A737 CaT. Nital etch, X500 (reduced 49% on reproduction)

Table 3 shows the improvement in tensile properties resulting from inclusion control. This improvement is most clearly shown in the reduction of area values in the S orientation. The benefits of inclusion control to A516 steel were established in previous work (Ref. 5, 7). The tensile properties of the A737 plate indicate improved yield strength properties over the A516 plates. Also, there appears to be a general improvement in the ductility of this steel over A516 in all testing orientations. These comparisons have been noted previously (Ref. 6).

Impact Toughness Properties

Charpy V-notch (CVN) impact properties of these four plates were determined using standard 10 mm (0.39 in.) square specimens per ASTM E23. Testing was conducted in three orientations: longitudinal (LT), transverse (TL), and through-thickness (ST). The ST orientation specimens were obtained from 0.5 in. (13 mm) plates by friction welding studs to plate blanks to allow full size CVN specimens

Table 4—Base Metal Charpy V-Notch Impact Properties

		USE[(a)]		−50°F (−46°C)[(b)]	
Material	Orient.	Ft-lb	(J)	Ft-lb	(J)
A516 CON	LT	65	(88)	24	(33)
	TL	42	(57)	15	(20)
	ST	11	(15)	4	(5)
A516 ESR	LT	138	(187)	45	(61)
	TL	70	(95)	21	(28)
	ST	46	(62)	9	(12)
A516 CaT	LT	123	(167)	38	(52)
	TL	77	(104)	24	(33)
	ST	49	(66)	10	(14)
A737 CaT	LT	200	(271)	195	(264)
	TL	122	(165)	76	(103)
	ST	76	(103)	32	(43)

(a) USE—Upper shelf energy; average of 3-5 specimens at 100% ductile fracture.
(b) −50°F—Absorbed energy at −50°F (−46°C).

to be machined.

The CVN test results are presented as absorbed energy transition curves in Fig. 4, and specific values are summarized in Table 4. Once more the benefits of inclusion control in the three A516 plates are demonstrated. The CVN results for the A737 CaT plate show improved levels of upper shelf toughness in all orientations in comparison to the A516 CaT plate.

The CVN results for these four steels show differences in all three testing orientations. The most dramatic improvements are noted in the ST orientation. The A516 CON steel had 11 ft-lb (15J) upper shelf energy in the ST orientation, while the CaT and ESR steels showed over 40 ft-lb (54J) and the A737 CaT 76 ft-lb (103J). These comparisons demonstrate the improvement resulting from inclusion control as well as the benefits obtainable from the A737 steel.

Experimental Procedure

Friction Welding

Two basic variations of the friction welding process are in common usage. They are inertia friction welding and direct drive friction welding.

Inertia friction welding utilizes the energy stored in a flywheel to generate the heat at the faying surfaces. The rotating part is attached to the freewheeling flywheel, while the stationary part is thrust against it. When the energy that remains in the flywheel is no longer sufficient to shear the plastic metal at the interface, rotation abruptly ceases. Axial thrust, however, continues and causes slight, controlled additional upset. The variables are flywheel energy and axial thrust.

Direct drive friction welding offers greater latitude in process variables. Heating of faying surfaces is accomplished by rotating one part against the other, which is held stationary. Axial thrust is sufficient to produce enough contact to generate heating and to radially extrude metal. At a predetermined time in the cycle, the drive mechanism is declutched and rotation ceases. Concurrently, the axial thrust is increased to produce upsetting at the weld zone.

Specimen Preparation and Evaluation

To facilitate friction weld evaluation, plates of the various test materials previously described were fabricated into 5 in. (127 mm) OD × 0.5 in. (12.7 mm) thick wall pipe. The plates were rolled, seam welded, normalized 1 hour (h) at 1650°F (899°C) and cut to the lengths required for the weld coupons. Half the coupons were welded by inertia friction welding and half by direct drive friction welding. Preliminary test specimens of A516 CON and ESR were welded to establish "opti-

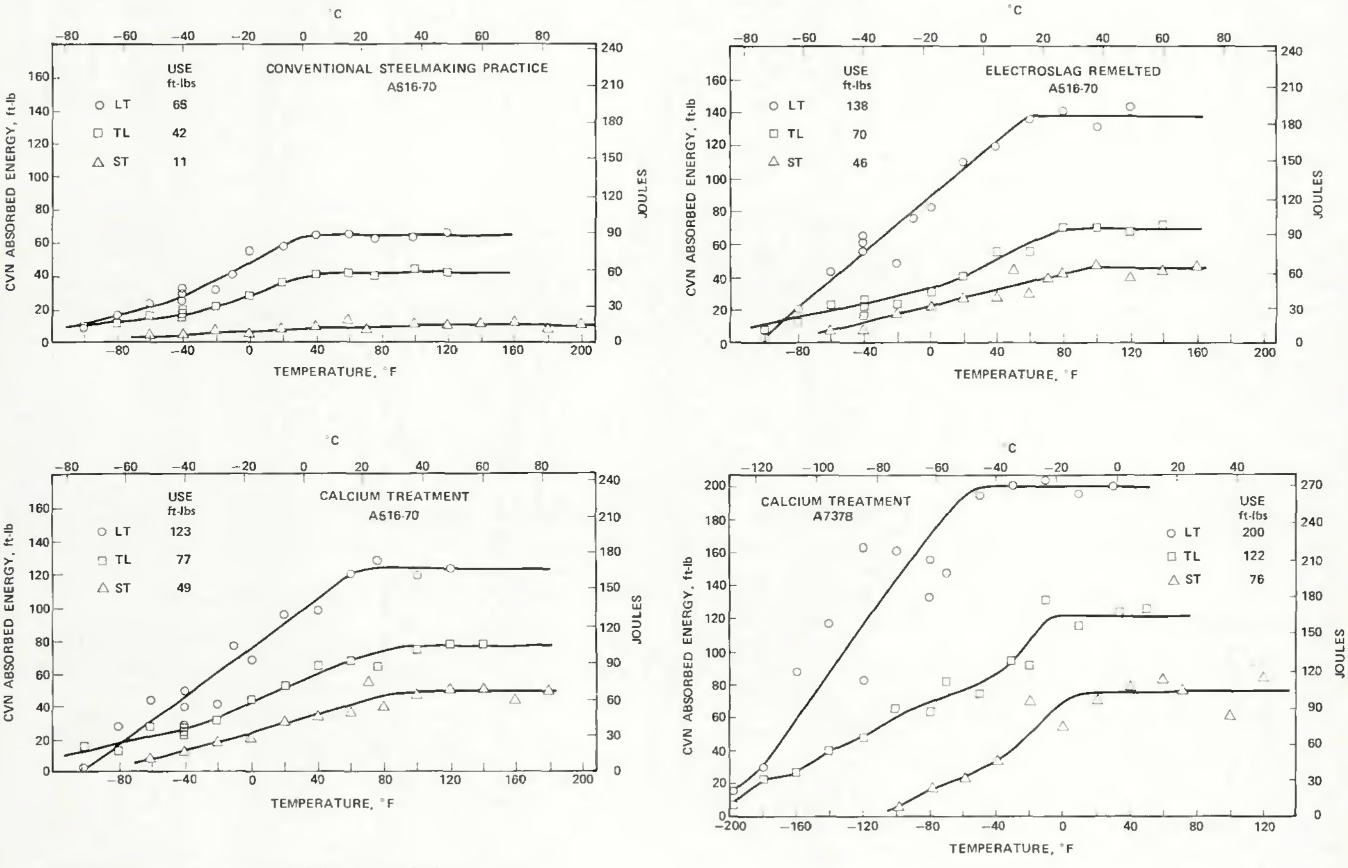

Fig. 4—CVN impact properties of base metal plates

mum" conditions for both processes. The optimization was based on impact tests at −40 and −50°F (−40 and −46°C) and on bend and tensile tests at room temperature.

The test results showed no significant differences between inertia and direct drive friction welds. The tensile strength and bend data did not discriminate among the conditions used for each process variation nor between them. The low temperature impact values were so low that any differences were well within experimental error. The final conditions ultimately were based on the experience of the users of each type of welding unit. The welding conditions established for the test program are given in Table 5. The weldments were not heat treated after welding.

Welds of each material were evaluated in accordance with Sections III (Nuclear Components) and IX (Weld Procedure Qualification) of the ASME Boiler and Pressure Vessel Code. Evaluation included tensile tests and bend tests through 180 deg. Impact testing was also performed, although the code does not require it, for material 0.625 in. (15.9 mm) or less in thickness. Full CVN transition curves were obtained. The CVN specimens were removed from the friction welded pipe so that the long axis of the specimen was parallel to the pipe axis. The notch was machined at the weld center line with the axis of the notch in the direction of the pipe radius. Impact was, therefore, in a direction which subjected the specimen to a side bend.

Test specimens were removed from the pipe sections by sawing or by water-injected plasma arc cutting to minimize heating of the specimen. The longitudinal seam welds were readily identified. The seam weld and associated heat-affected zone were removed and discarded.

Table 5—Friction Welding Conditions

Inertia	
Flywheel energy (WK^2)	2,224 lb-ft^2 (10,680 N-M^2)
Rotational speed	1873 SFM[(a)]
Upset force	127,332 lbf (57,880 N)
Upset (length loss)	~ 0.8 in. (20.3 mm)
Direct Drive	
Rotational speed	430 SFM[(a)]
Friction welding force	8,000 psi (55 MPa)
Friction upset distance	0.50 in. (12.7 mm)
Forge force	16,000 psi (110 MPa)
Total upset (length loss)	0.8 in. (20.3 mm)

(a) SFM—surface feet per minute.

Results

The mechanical properties anticipated from the earlier weld optimization tests were achieved. However, as mentioned earlier, a clear distinction between adequate and optimum conditions could not be made. There is evidence that optimum conditions were not attained, particularly for the direct drive friction welds. This is particularly noticeable in comparisons of the impact properties.

The results of the weld procedure qualification test are summarized in Table 6. All materials and processes passed the face bend test except the A516 CON material. Both this material and the A516 CaT had failures in the root bend test. All materials and processes passed tensile tests.

The Charpy V-notch curves are shown in Fig. 5. In this study, impact toughnesses of the inertia friction welds in the transition area were better than those for the direct drive friction welds. This is particularly shown at the −40°F (−40°C) test temperature. In two instances useful toughness at −40°F (−40°C) was achieved: 12 ft-lb (16J) for the inertia welded A516 CaT and 20 ft-lb (27J) for the inertia welded A737 CaT.

As the test temperature increased, the benefits of inclusion control became more apparent in the A516 comparisons, particularly for the inertia friction welds. These comparisons are best shown in Fig. 6 for the inertia friction welds of the four materials. Figure 6 shows that the largest gains for inclusion control are indicated on the CVN upper shelf. This is further shown in Table 7, where the upper shelf energies for the inertia friction welds of these four materials are compared. Figure 6 and Table 7 also indicate that the A737 CaT material provides the best toughness in the inertia friction weld over the full range of temperatures.

Table 6—Weld Mechanical Test Results

	Bend angle deg		Tensile properties[(d)]			
Process and material	Face	Root	YS, ksi	UTS, ksi	El, %	Fracture location
Continuous Drive						
A516 CON	20[(a)]	15[(a)]	56	82	16	Weld
A516 CON	20[(a)]	180	55	83	20	Weld
A516 ESR	180	180	56	82	31	Base metal
A516 ESR	180	180	54	83	31	Base metal
A516 CaT	180	180	59	80	16	Edge of weld
A516 CaT	180	180	51	80	19	Edge of weld
A737 CaT	180	180	55	75	30	Base metal
A737 CaT	180	180	54	75	33	Base metal
Inertia						
A516 CON	180	30[(a)]	52	83	28	Base metal
A516 CON	180[(b)]	180	50	81	25	Base metal
A516 ESR	180	180	57	84	33	Base metal
A516 ESR	180	180	58	84	30	Base metal
A516 CaT	180	15[(c)]	49	79	28	Base metal
A516 CaT	180	15[(c)]	54	78	28	Base metal
A737 CaT	180	180	57	77	33	Base metal
A737 CaT	180	180	56	76	33	Base metal

(a) Failed; less than 180 deg before cracking; cracks at weld center line.
(b) Failed; cracks greater than ⅛ in. (3.2 mm) long; cracks at weld center line.
(c) Failed; less than 180 deg before cracking; cracks not at weld center line.
(d) YS—yield strength; UTS—ultimate tensile strength; El—elongation.

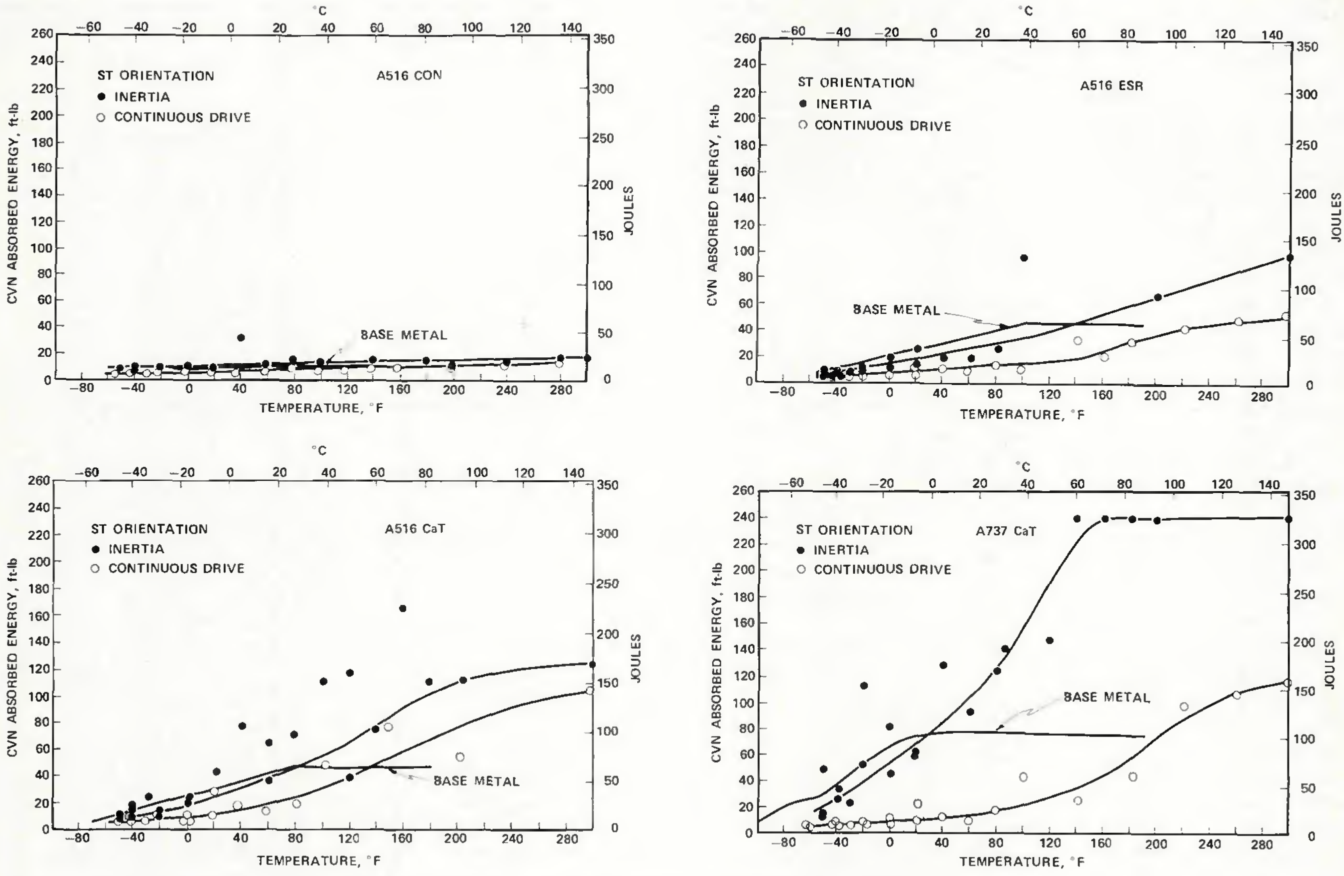

Fig. 5 — Impact properties of friction welds compared to properties of the base metal in ST orientation

Microstructures of the weld metal differ markedly from the wrought base metal. There are also significant differences between welds made by the two processes. The base metal has the banded structure typical of rolled plate. The grain size of the A516 materials was coarser than that of the A737 CaT.

The microstructures of the weld metal and the corresponding base metal are shown in Fig. 7. Both weld types exhibit a bainitic acicular structure. The inertia friction welds had a fine microstructure, while the corresponding direct drive friction weld metal had a coarser structure. A comparison of the width of these solid-state welds (actually heat-affected zones) is shown in Fig. 8. Note that the direct drive welds are broader.

Microhardness traverses were obtained across the welds of all steels. In all four test materials the peak Knoop hardness of the inertia friction welds was significantly higher than that of the direct drive friction welds; this was a result consistent with what would be expected for the finer bainitic structure noted above. A comparison of A516 CaT and A737 CaT, for the two friction welding process variations, is shown in Fig. 9.

Table 7—Upper Shelf Energy at 300°F (65°C) for Friction Welds, ft-lb

Material	Inertia	Direct drive
A516 CON	14	14
A516 ESR	94	49
A516 CaT	127	105
A737 CaT	240[a]	116

[a] Exceeded capacity of the testing machine.

The fracture surfaces from upper shelf CVN tests of friction welds were examined using scanning electron microscopy. The inclusions found on the A516 CON surface tended to be large MnS inclusions; the other materials tended to show smaller and fewer inclusions as shown in Fig. 10 for A516 CON and A516 CaT.

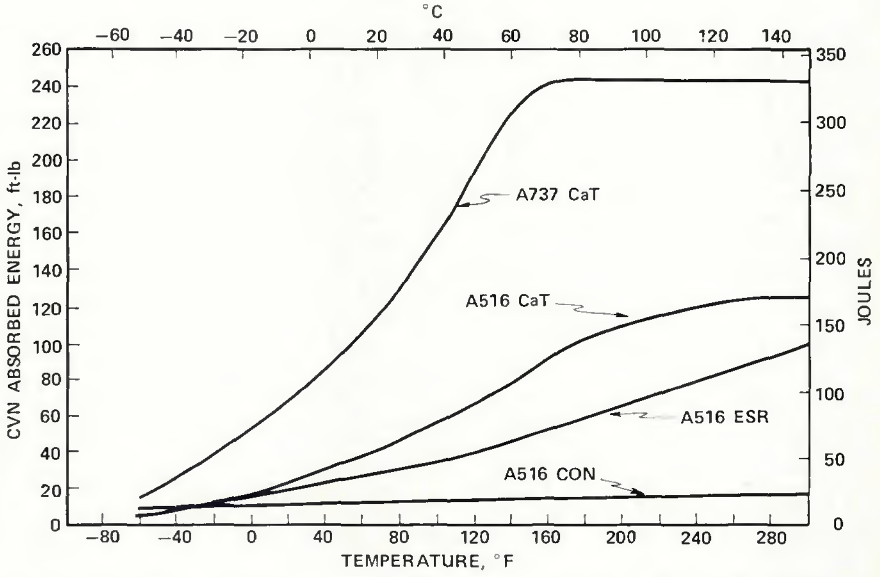

Fig. 6 — Impact of inertia friction welds showing improvement in toughness obtained through inclusion control

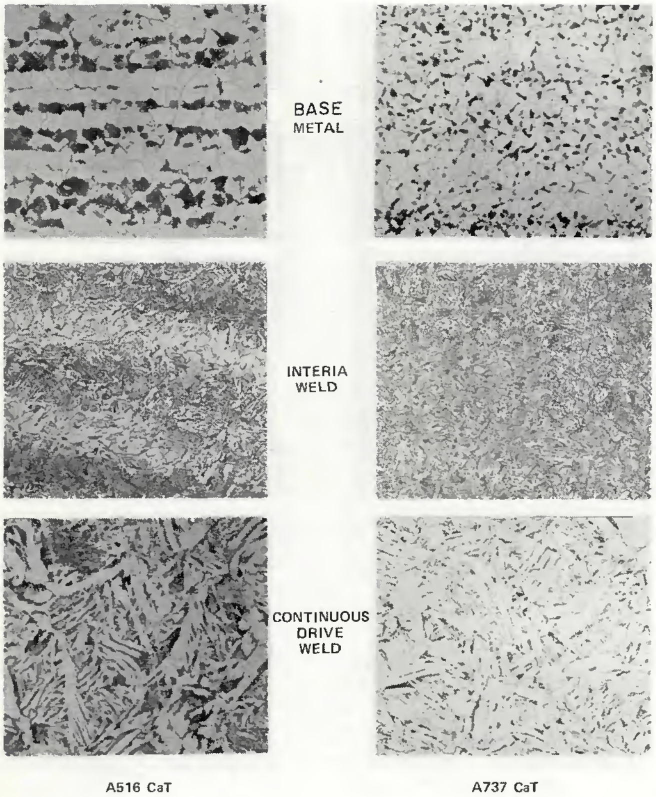

Fig. 7 — Comparison of weld metal and base metal microstructures for A516 CaT and A737 CaT steels. Nital etch; ×500 (reduced 50% on reproduction)

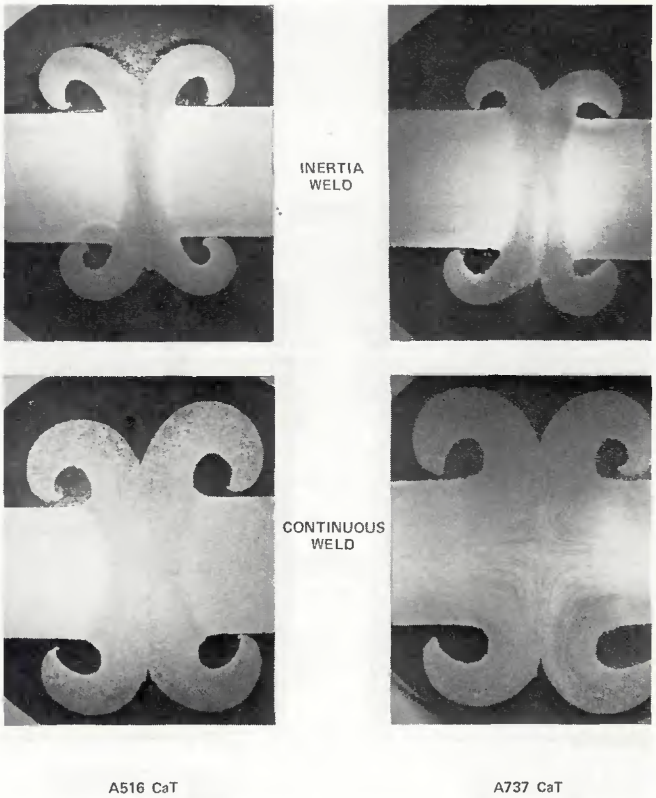

Fig. 8 — Comparison of heat-affected zones for inertia and direct drive friction welds in A516 CaT and A737 CaT steels. Picral etch, ×4 (reduced 47% on reproduction)

Discussion

In this program the weld test results varied, depending on the type of friction welding process variation and the type of test. Charpy V-notch (CVN) impact properties were of greatest interest. The friction weld CVN properties can be compared to base metal properties. Generally, the friction weld impact transitions were shifted to higher temperatures when compared to base metal transitions. The upper shelf* region of the CVN curves for the friction welds tended to follow the upper shelf curves for the ST orientation of the base metal more closely than for the LT or TL orientations. The friction weld upper shelf energy, however, was generally higher than the ST orientation upper shelf energy of the base metal. It appears that the impact toughness of a friction weld can be predicted best from impact toughness of base metal samples having the ST orienta-

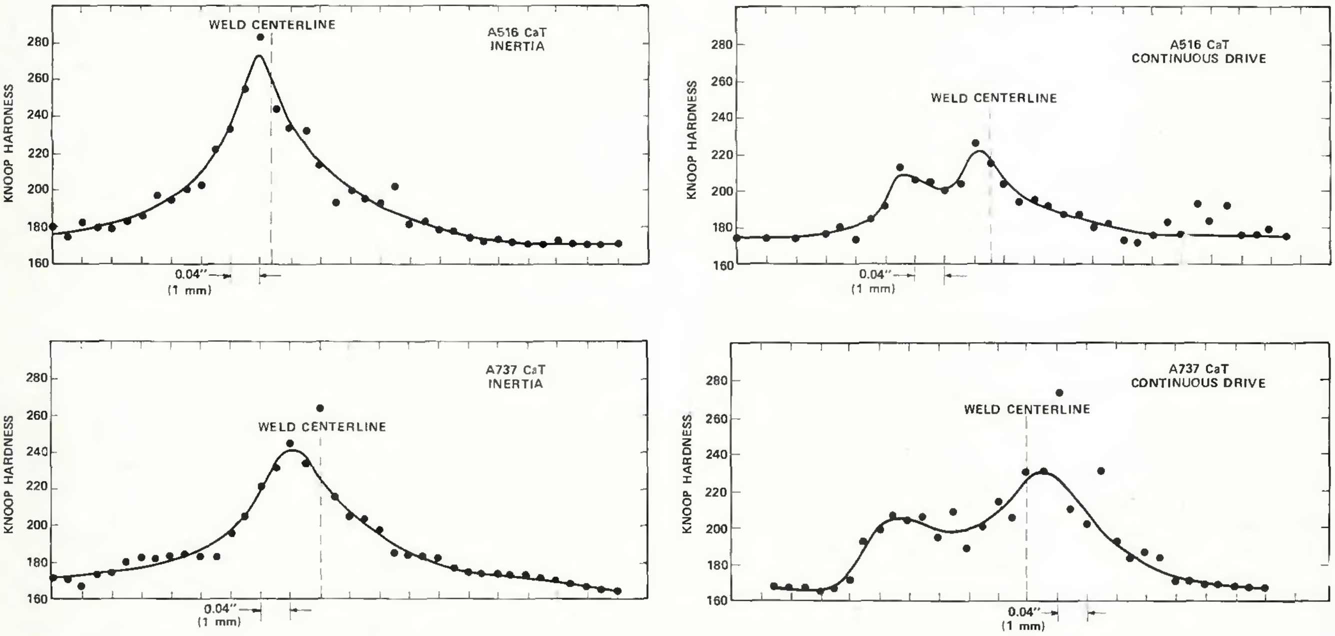

Fig. 9 — Microhardness traverses across the weld zone for inertia and continuous drive welds in A516 CaT and A737 CaT steels

---

**Upper shelf — the upper limits of Charpy impact transition curves where a leveling off is observed when plotting impact values vs. test temperatures.*

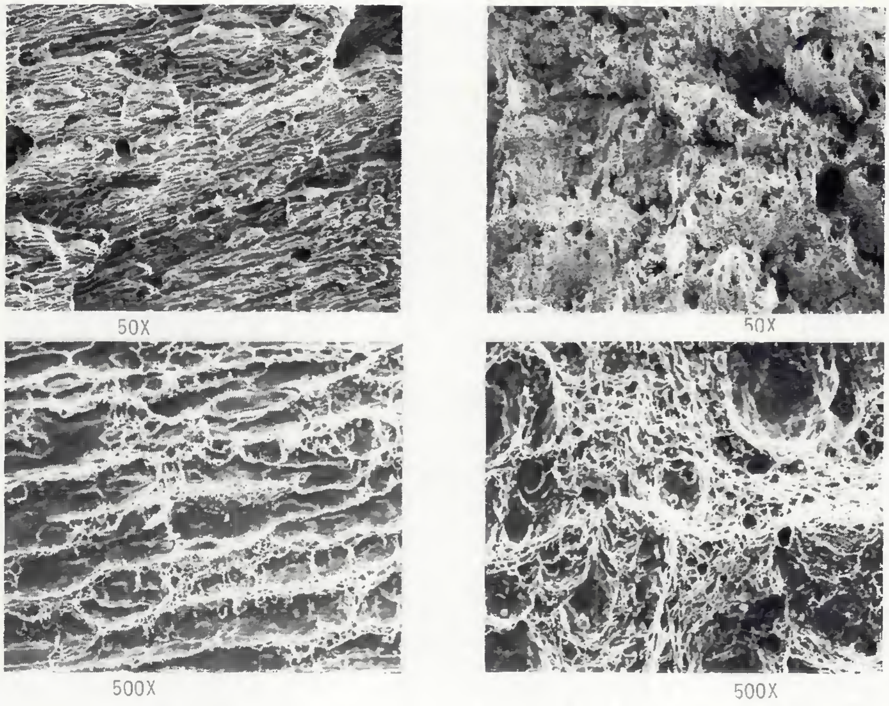

A516 CON **A516 CaT**

Fig. 10 — Fracture surface of friction welds in A516 CON and A516 CaT steels. The A516 CON fracture is predominately cleavage with remnants of platelike inclusions very evident. In contrast, the A516 CaT fracture is totally ductile with nearly spherical inclusions evident at site of void formation (reduced 30% on reproduction)

tion.

The single most important contribution of this program was toward understanding the influence of inclusion control on friction weld properties. This is particularly indicated on the upper shelf of the CVN curve. The results of the testing of the three A516 plates showed the superior toughness of the inclusion controlled steels, such as CAT and ESR.

The results of testing certainly support the initial hypothesis of this program — namely, that nonmetallic inclusions are rotated into the eventual plane for CVN testing of friction weldments. Therefore, the lowering of inclusion content and modifying of inclusion structure tended to improve the ductility and toughness of friction welds. The presence of inclusions on the fracture surfaces as noted by the SEM fractography also supported this conclusion.

The A737 CaT steel showed the best overall friction weld properties in this test program. The fine grain size and lower carbon content of this steel led to improved transition temperature and upper shelf toughness of the friction welds. Although the fine grain size of the base metal was not strictly maintained in the friction weld, the structure was refined in comparison to the A516, thus leading to the improved transition area toughness of this grade of steel.

For a given welding process, the microhardness results for the A737 and the A516 were similar. This also indicates that, even though the carbon content was lower for the A737 (0.12 vs. >0.20 for the A516 steels), the finer grain size of the A737 is maintained and gives similar weldment strength levels.

The comparison of the friction weld process variations generally indicated property differences, particularly in CVN toughness. In this study, the friction weld CVN toughness in the transition area was better for the inertia friction welds than for the direct drive friction welds. This was found to be due to the greater heat input used in the direct drive process, as indicated by the coarser bainitic structure in these welds and the broader heat-affected zone.

The results of this comparison indicate that possibly the welding conditions used in the direct drive variation were not fully optimized. It further suggests that varying the heat input during friction welding can have a significant influence on the ductility and the toughness of the resulting weldment.

Conclusions

1. Inclusion control by calcium treatment or electroslag remelting significantly improved the ductility and toughness of friction weldments.

2. The ductility and toughness of the friction welds from A737 steel were found to be superior to those for A516, reflecting the superior properties of the base metal for this grade.

3. The Charpy V-notch toughness of friction welds appeared to correlate with the base metal CVN properties tested in the through-thickness orientation.

4. In the context of this study, the welds prepared by inertia friction welding were tougher than those obtained by direct drive friction welding. This is apparently a result of the significantly greater heat input used in the direct drive process variation for this program.

Acknowledgments

This program was conducted under the auspices of the AWS C6 Committee on Friction Welding. A number of individuals and firms were involved. In particular, the authors wish to thank Lukens Steel Co. for the steel plate and D. E. Spindler of Manufacturing Technology, Inc., and S. B. Carlson of New Britain Machine for providing assistance and facilities for the inertia and continuous drive welding, respectively. Credit is also given to C. B. Jones and J. W. Kelker, Jr., E. I. du Pont de Nemours, Aiken, S. C., for providing the initial planning and guidance for this project.

It is to be noted that the Savannah River Plant is operated for the U.S. Department of Energy by E. I. du Pont de Nemours and Co., Inc. under contract DE-AC09-76SR00001.

References

1. Shappert, L. B. 1970 (Feb.). *Cask designer's guide.* ORNL-NSIC-68, Nuclear Safety Information Center, ORNL.

2. Barrert, J. C. 1945. Flash welding of alloy steels — physical and metallurgical characteristics. *Welding Journal* 24(1): 13-s to 32-s.

3. Savage, W. F. 1962. Flash welding — the process and application. *Welding Journal* 41(3): 227-237.

4. Savage, W. F. 1962. Flash welding — process variables and weld properties. *Welding Journal* 41(3): 109-s to 119-s.

5. Wilson, A. D. 1979. *The effect of advanced steel making techniques on the inclusion and mechanical properties of plate steels, toughness characterization and specifications for HSLA and structural steels.* ed. P. L. Mangonon, Jr., TMS-AIME.

6. Wilson, A. D. 1980 (July). The fatigue and toughness properties of a C-Mn-Cb plate steel. *Transactions of ASME: Journal of Engineering Materials and Technology.* 102: pp 269-279.

7. Wilson, A. D. 1979 (July). The influence of inclusions on the toughness and fatigue properties of A516-70 steel. *Transactions of the ASME. Journal of Engineering Materials and Technology.* 101, pp 265-274.

8. Dinsdale, W. O., and Dunkerton, S. B. 1981 (Sept.). *The impact properties of forge butt welds in carbon-manganese steels — part I: continuous drive friction welds.* Research report no. 159/1981. Cambridge, England: The Welding Institute.

9. Dinsdale, W. O., and Dunkerton, S. 8. 1981 (Sept.). The impact properties of forge butt welds in carbon-manganese steels — part II: *orbital friction and inertia welds.* Research report no. 160/1981. Cambridge, England: The Welding Institute.